

# Four decades of water quality change in the upper San Francisco Estuary

Marcus W. Beck<sup>1\*</sup>, Thomas W. Jabusch<sup>2</sup>, Philip R. Trowbridge<sup>2</sup>, David B. Senn<sup>2</sup>

*\*Corresponding author: [marcusb@sccwrp.org](mailto:marcusb@sccwrp.org)*

*<sup>1</sup>USEPA National Health and Environmental Effects Research Laboratory  
Gulf Ecology Division, 1 Sabine Island Drive, Gulf Breeze, FL 32561*

*Current address: Southern California Coastal Water Research Project  
3535 Harbor Blvd, Suite 110, Costa Mesa, CA 92626*

*<sup>2</sup>San Francisco Estuary Institute  
4911 Central Ave, Richmond, CA 94804*

Version Date: Fri Oct 6 15:33:58 2017 -0700

## ***Abstract***

Historical trends and relationships between key species of dissolved inorganic nitrogen (ammonium, nitrate/nitrite, total) from the Delta region of the San Francisco Estuary (SFE) were modeled with an estuarine adaptation of the Weighted Regressions on Time, Discharge, and Season (WRTDS). Trend analysis with flow-normalized results demonstrated the potential to misinterpret changes using observed data that included flow effects, such that several trends with flow-normalized data had changes in magnitude and even reversal of trends relative to the observed. We further described mechanisms of change with two case studies that evaluated 1) downstream changes in nitrogen following upgrades at a wastewater treatment plant, and 2) interactions between biological invaders, chlorophyll, and flow in Suisun Bay. WRTDS results for ammonium trends showed a distinct signal as a result of upstream wastewater treatment plant (WWTP) upgrades, with specific reductions observed in the winter months during low-flow conditions. Results for Suisun Bay showed that chlorophyll *a* (chl-*a*) production in early years was directly stimulated by flow, whereas the relationship with flow in later years was indirect and confounded by grazing pressure. Although these trends and potential causes of change have been described in the literature, results from WRTDS provided an approach to test alternative hypotheses of spatiotemporal drivers of nutrient dynamics in the Delta.

## ***1 Introduction***

The Sacramento - San Joaquin River Delta (hereafter 'Delta') is a mosaic of inflows upstream of the San Francisco Estuary (SFE) that receives and processes inputs from the highly agricultural watershed of the Central Valley (Jassby and Cloern 2000, Jassby et al. 2002, Jassby

25 2008). Sediment transport and wastewater treatment plant (WWTP) inputs from the Delta are  
26 primary sources of nutrients for the larger Bay (Dugdale et al. 2007, Cornwell et al. 2014).  
27 Although water quality conditions in SFE symptomatic of eutrophication have historically been  
28 infrequent, changes in response to stressors suggests that recent conditions have not followed past  
29 trajectories. Increases in phytoplankton biomass, reductions in dissolved oxygen, and increasing  
30 abundance of species associated with harmful algal blooms have been a recent concern for the  
31 management of this prominent system (Lehman et al. 2005, Cloern et al. 2005, Shellenbarger  
32 et al. 2008, Cloern et al. 2007). As a result, chlorophyll *a* (chl-*a*) thresholds to assess and manage  
33 levels of concern for phtoplankton biomass in the lower bay have been proposed (Sutula et al.  
34 2017). Although these changes are linked to drivers at different spatial and temporal scales, inputs  
35 from the Delta remain a critical interest for understanding downstream effects.

36 Nutrient concentrations are generally non-limiting for phytoplankton growth in the upper  
37 SFE. In contrast, light conditions have long been considered the primary limiting factor  
38 preventing accumulation of phytoplankton biomass (Cole and Cloern 1984, Alpine and Cloern  
39 1988), whereas grazing pressure from pelagic and benthic species can reduce phytoplankton  
40 during periods of growth (Nichols 1985, Jassby 2008, Kimmerer and Thompson 2014).  
41 Moreover, changes in flow management practices compounded with climate variation have  
42 altered flushing rates and turbidity as key factors that moderate phytoplankton growth in the  
43 system (Alpine and Cloern 1992, Lehman 2000, Wright and Schoellhamer 2004, Canuel et al.  
44 2009). Glibert et al. (2014) described recent phytoplankton blooms in Suisun Bay that were  
45 attributed to increased residence times and increased rates of nitrification that occurred during a  
46 drought period. Speciation changes in the dominant forms of nitrogen are considered key factors  
47 that contribute to phytoplankton blooms, particularly seasonal reductions in ammonium that allow

uptake of nitrate that stimulates growth (Dortch 1990, Dugdale et al. 2007). Changes in phytoplankton biomass and the effects on pelagic organisms have also been of concern. Jassby (2008) described decadal trends in phytoplankton biomass to understand mechanisms of decline for pelagic fish populations in the Delta. Although phytoplankton concentrations have been relatively consistent in Suisan Bay, biomass in the upper Delta has been increasing. Much of these trends were explained by invasion of benthic grazers in polyhaline areas and changes in the mean flow conditions observed in the Delta.

A comprehensive water quality monitoring program has been in place in the Delta for several decades (IEP 2013). Although these data have been used extensively, a systematic assessment of trends covering the full spatial and temporal coverage of the monitoring dataset has not been made. This information could inform both past and current research by providing a cohesive description of system-wide trends in nutrients. However, formal methods for trend analysis are required given that long-term changes can be masked by variation at shorter time scales or the observed variation represents the combined effects of many variables (O'Neill et al. 1989, Levin 1992). As a practical approach for water quality evaluation, trend analysis of ecosystem response indicators often focuses on tracking the change in concentrations or loads of nutrients over many years. Response indicators can vary naturally with changing flow conditions and may also reflect long-term effects of management or policy changes. For example, chl-*a* concentration as a measure of phytoplankton response to nutrient inputs can follow seasonal patterns with cyclical variation in temperature and light changes throughout each year, whereas annual trends can follow long-term variation in nutrient inputs to the system (Cloern 1996, Cloern and Jassby 2010). Similarly, nutrient trends that vary with hydrologic loading also vary as a function of utilization rates by primary producers or decomposition processes (Sakamoto and

Tanaka 1989, Schultz and Urban 2008, Harding et al. 2016).

The Weighted Regressions on Time, Discharge, and Season (WRTDS) approach was developed in this context and has been used to characterize decadal trends in running-water systems (Hirsch et al. 2010, Sprague et al. 2011, Medalie et al. 2012, Hirsch and De Cicco 2014, Pellerin et al. 2014, Zhang et al. 2016). The WRTDS method has been adapted for trend analysis in tidal waters, with a focus on chl-*a* trends in Tampa Bay (Beck and Hagy III 2015) and the Patuxent River Estuary (Beck and Murphy 2017). The goal of this study was to provide a comprehensive description of nutrient trends in the northern SFE and Delta region to inform understanding of ecosystem response dynamics and potential causes of water quality change. The specific objectives were to 1) quantify and interpret trends over four decades at ten stations in the Delta, including annual, seasonal, and spatial changes in nitrogen analytes and response to flow variation, and 2) provide detailed descriptions of two case studies in the context of conceptual relationships modeled with WRTDS. The second objective evaluated two specific water quality stations to demonstrate complexities with nutrient response to flow, effects of nutrient-related source controls on ambient conditions, and effects of biological invasion by benthic filter feeders on primary production. Our general hypothesis was that the results were expected to support previous descriptions of trends in this well-studied system, but that new insight into spatial and temporal variation in response endpoints was expected, particularly in flow-normalized model predictions.

## 2 *Materials and Methods*

### 2.1 Study system

The Delta region drains a 200 thousand km<sup>2</sup> watershed into the SFE, which is the largest estuary on the Pacific coast of North America. The watershed provides water to over 25 million people and irrigation for 18 thousand km<sup>2</sup> of agricultural land. Water enters the SFE through the Sacramento and San Joaquin rivers that have a combined inflow of approximately 28 km<sup>3</sup> per year, with the Sacramento accounting for 84% of inflow to the Delta. The SFE system includes the Delta and subembayments of San Francisco Bay (Fig. 1). Water dynamics in the SFE and Delta are governed by inflows from the watershed, tidal exchange with the Pacific Ocean, and water withdrawals for municipal and agricultural use (Jassby and Cloern 2000). Seasonally, inflows from the watershed peak in the spring and early summer from snowmelt, whereas consumption, withdrawals, and export have steadily increased from 1960 to present, but vary depending on inter-annual climate effects (Cloern and Jassby 2012). Notable drought periods have occurred from 1976-1977, 1987-1992, and recently from 2013-2015 (Cloern 2015).

Orthophosphate ( $\text{PO}_4^{3-}$ ) and dissolved inorganic nitrogen (DIN) enter the Delta primarily through the Sacramento and San Joaquin rivers and from municipal WWTP inputs. Annual nutrient export from the Delta region has been estimated as approximately 30 thousand kg d<sup>-1</sup> of total nitrogen (varying with flow, Novick et al. 2015), with 90% of ammonium ( $\text{NH}_4^+$ ) originating solely from the Sacramento Regional WWTP (Jassby 2008). Although nitrogen and phosphorus inputs are considerable, primary production is relatively low and not nutrient-limited (Jassby et al. 2002, Kimmerer et al. 2012). The resistance of SFE to the negative effects of eutrophication has

historically been attributed to its unique physical and biological characteristics, including strong tidal mixing that limits stratification in the larger estuary (Cloern 1996, Thompson et al. 2008) and limits on phytoplankton growth from high turbidity and filter-feeding by bivalve mollusks in the northern portion (Thompson et al. 2008, Crauder et al. 2016). However, recent water quality trends have suggested that resilience to nutrient inputs is decreasing (Lehman et al. 2005, Cloern et al. 2007, Lehman et al. 2010), which has been attributed to biological invasions (Cohen and Carlton 1998) and departures from the historical flow record (Enright and Culberson 2009, Cloern and Jassby 2012), among other factors acting at global scales (e.g., variation in sea surface temperatures, Cloern et al. 2007).

Quantitative descriptions of nutrient dynamics in the Delta are challenging given multiple sources and the volume of water that is exchanged with natural and anthropogenic processes. A comprehensive evaluation using mass-balance models to describe nutrient dynamics in the Delta demonstrated that nitrogen enters the system in different forms and is processed at different rates before export or removal (Novick et al. 2015). For example, a majority of ammonium entering the system during the summer is nitrified or assimilated, whereas a considerable percentage of total nitrogen load to the Delta is exported. Although, the focus of our analysis is not to quantify sources or sinks of nitrogen species, a quantitative evaluation of long-term trends will provide a more comprehensive historical interpretation to hypothesize the effects of future changes in the context of known dynamics. Nutrients in the Delta also vary with seasonal and annual changes in the delivery of water inflows and water exports directly from the system (Jassby and Cloern 2000, Jassby 2008). Our analysis explicitly accounts for the effects of flow changes on nutrient response to better understand variation both within the Delta and potential mechanisms of downstream transport.

## 2.2 Data sources

Nutrient time series of monthly observations from 1976 to 2013 were obtained for ten active sampling stations in the Delta (Fig. 1, <http://water.ca.gov/bdma/meta/Discrete/data.cfm>, IEP (2013)). Stations were grouped by location in the study area for comparison: peripheral Delta stations C3 (Sacramento inflow), C10 (San Joaquin inflow), MD10, P8; interior Delta stations D19, D26, D28; and Suisun stations D4, D6, and D7. These stations cover all of the major inflows and outflows to the Delta and were selected for analysis based on the continuity of the period of observation (Jabusch and Gilbreath 2009). Although many other stations are available for the region, the stations were chosen because they are actively maintained by the regional monitoring program and they capture dominant seasonal and annual modes of nitrogen variability characteristic of the region (Jabusch et al. 2016). Time series were complete for all stations except for an approximate ten year gap from 1996-2004 for D19. Data were minimally processed, with the exception of averaging replicates that occurred on the same day. The three nitrogen analytes that were evaluated were ammonium, nitrite/nitrate, and DIN (as the sum of the former two). Less than 3% of all observations were left-censored, although variation was observed between analytes and location. The ammonium time series had the most censored observations at sites C10 (25.4% of all observations), MD10 (18.1%), D28 (17.8%), D19 (12%), and D7 (7.9%).

Daily flow estimates for the Delta region were obtained from the Dayflow software program (IEP 2016). The WRTDS models described below require a matched flow record with the appropriate station to evaluate nutrient trends. Given the complexity of inflows and connectivity of the system, only the inflow estimates from the Sacramento and San Joaquin rivers were used as measures of freshwater influence at each station. Initial analyses indicated that



model fit was not significantly improved with flow estimates from locations closer to each station, nor was model fit improved using lagged times series. As such, the Sacramento daily flow time series was used to account for flow effects at C3, D19, D26, D28, and MD10, and the San Joaquin time series was used for C10 and P8 based on station proximity to each inflow. Salinity observations at D4, D6, and D7 in Suisun Bay were used as more appropriate measures of freshwater variation, given the stronger tidal influence at these stations. Salinity has been used as a tracer of freshwater influence for the application of WRTDS models in tidal waters (Beck and Hagy III 2015).

### 2.3 Analysis method and application

A total of thirty WRTDS models were created, one for each nitrogen analyte at each station. The functional form of WRTDS is a simple regression (Hirsch et al. 2010) that models the log-transformed response variable as a function of time, flow, and season:

$$\ln(N) = \beta_0 + \beta_1 t + \beta_2 \ln(Q) + \beta_3 \sin(2\pi t) + \beta_4 \cos(2\pi t) \quad (1)$$

where  $N$  is one of three nitrogen analytes, time  $t$  is a continuous variable as decimal time to capture the annual or seasonal trend, and  $Q$  is the flow variable (either flow or salinity depending on station). Generally, the WRTDS model is a moving window regression that fits unique parameters at each observation point in the time series. Rather than fitting a global model to the entire time series, one regression is fit at every point in the time series. Observations within a window used to fit each regression are weighted relative to annual, seasonal, and flow distances from the center of the window. Observations with distances farther from the center (i.e., greater time and different flow values from the center) have less weight during parameter estimation for

each regression. This approach allows for a type of smoothing where the observed fit is specific to each point in the time series. Models applied herein were based on a tidal adaptation of the original method that can use either flow or salinity estimates as nutrient predictors (Beck and Hagy III 2015). All models were fit to describe the conditional mean response using a weighted Tobit model for left-censored data (Tobin 1958). Model predictions were evaluated as monthly values or as annual values that averaged monthly results within each water year (October to September). All analyses used the WRTDStidal package for the R statistical programming language (Beck 2017, RDCT (R Development Core Team) 2017).

A hallmark of the WRTDS approach is the description of flow-normalized trends that are independent of variation from freshwater inflows (Hirsch et al. 2010). Flow-normalized trends for each analyte at each station were used to describe long-term changes in different annual and seasonal periods. Flow-normalization predictions for each month of each year were based on the average of predictions for flow values that occur in the same month across all years, weighted within each specific month and year for every observation. Flow-normalized trends in each analyte were summarized as both medians and percent changes from the beginning to end of annual groupings from 1976-1995 and 1996-2013, and seasonal groupings of March-April-May (spring), June-July-August (summer), September-October-November (fall), and December-January-February (winter) within each annual grouping. These annual and seasonal groupings were chosen for continuity with similar comparisons in Jabusch et al. (2016) and as approximate twenty year midpoints in the time series.

Trends in each annual and seasonal grouping were based on seasonal Kendall tests of the flow-normalized predictions. This test is a modification of the non-parametric Kendall test that accounts for variation across seasons in the response variable (Hirsch et al. 1982, Millard 2013).

Results from the test can be used to evaluate the direction, magnitude, and significance of a monotonic change within the period of observation. The estimated rate of change per year is also returned as the Theil-Sen slope and was interpreted as the percent change per year when divided by the median value of the response variable in the period of observation (Jassby 2008). Trends in annual groupings were based on all monthly observations within relevant years, whereas seasonal groupings were based only on the relevant months across years. Seasonal Kendall tests were also used to describe trends in the observed data. These trends were compared with those based on the flow-normalized trends to evaluate the improved ability of WRTDS to describe trends that are independent of flow.

### 3 Results

#### 3.1 Observed Data

The observed time series for the ten Delta - Suisun Bay stations had substantial variation in scale among the nitrogen analytes and differences in apparent seasonal trends (Fig. 2). DIN for most stations was dominated by nitrite/nitrate, whereas ammonium was a smaller percentage of the total. However, C3 had a majority of DIN composed of ammonium and other stations (e.g., P8, D26) had higher concentrations of ammonium during winter months when phytoplankton assimilation is lower (Novick et al. 2015). By location, observed concentrations of DIN for the entire time series were higher on average for the peripheral stations (C3, C10, MD10, P8; mean  $\pm$  s.e.:  $1.04 \pm 0.03$  mg L<sup>-1</sup>) and similar for the interior (D19, D26, D28,  $0.43 \pm 0.01$ ) and Suisun Bay stations (D4, D6, D7,  $0.44 \pm 0.01$ ). Average concentrations were highest at P8 ( $1.63 \pm 0.05$  mg L<sup>-1</sup>) and lowest at C3 ( $0.4 \pm 0.01$ ) for DIN, highest at P8 ( $0.28 \pm 0.02$ ) and lowest at D28 ( $0.05 \pm 0.003$ ) for ammonium, and highest at C10 ( $1.4 \pm 0.04$ ) and lowest at C3 ( $0.15 \pm 0.004$ ) for

nitrite/nitrate. Mean observed concentrations were also higher later in the time series for all analytes. For example, average DIN across all stations was  $0.61 \pm 0.01$  mg L<sup>-1</sup> for 1976-1995, compared to  $0.7 \pm 0.01$  for 1996-2013. Seasonal changes across all years showed that nitrogen concentrations were generally lower in the summer and higher in the winter, although observed patterns were inconsistent between sites. For example, site MD10 had distinct seasonal spikes for elevated DIN in the winter, whereas other stations had less prominent seasonal maxima (e.g., C3, D7, Fig. 2).

### 3.2 Trends

Estimated trends from Seasonal Kendall tests on the observed data varied considerably between sites and analytes (Fig. 4). Significant trends were observed from 1976-1995 for eight of ten sites for DIN (seven increasing, one decreasing), eight sites for ammonium (six increasing, two decreasing), and six sites for nitrite/nitrate (five increasing, one decreasing). Decreasing trends were more common for the observed data from 1996-2013. Eight sites had significant trends for DIN (four increasing, four decreasing), seven sites for ammonium (five increasing, two decreasing), and eight sites for nitrite/nitrate (four increasing, four decreasing). P8 had a relatively large decrease in ammonium ( $-8.3\%$  change per year) for the second annual period compared to all other sites (see next section). Trends by season were similar such that increases were generally observed in all seasons from 1976-1995 (Fig. 5) and decreases were observed for 1996-2013 (Fig. 6). Trends for the seasonal comparisons were noisier and significant changes were less common compared to the annual comparisons.

Relationships between flow and observed water quality are complex and can change significantly through space and time (Hirsch et al. 2010, Zhang et al. 2016). These principles have

been demonstrated for monitoring data in the Delta region (Jassby 2008, Novick et al. 2015, Jabusch et al. 2016), suggesting that trend analyses using the observed time series are confounded by flow effects. As such, a comparison of flow-normalized results from WRTDS relative to observed data identified changes in the magnitude, significance, and direction of trends. For all sixty trend comparisons in Fig. 4 (flow-normalized values in Table 1) regardless of site, nitrogen analyte, and time period, thirteen comparisons had trends that were insignificant with the observed data but significant with flow-normalized results, whereas only one trend changed to insignificant. This suggests that time series that include flow effects had sufficient noise to obscure or prevent identification of an actual trend of a water quality parameter. Further, changes in the magnitude of the estimated percent change per year were also apparent for the flow-normalized trends, such that fourteen comparisons showed an increase in magnitude (more negative or more positive) and twenty five had a decrease (less positive or less negative) compared to observed trends. Eleven comparisons showed a trend reversal from positive to negative estimated change, nine sites went from no change to negative estimated change, and one site went from no change to a positive trend for the flow-normalized results. Differences by season in the observed relative to flow-normalized trends from WRTDS were also apparent (Figs. 5 and 6 and Tables 2 and 3). The most notable changes were an overall decrease in the estimated trend for most sites in the summer and fall seasons for 1996-2013, including an increase in the number of statistically significant trends.

### 3.3 Selected examples

Two stations were chosen to demonstrate use of WRTDS to develop a more comprehensive description of decadal trends in the Delta. The selected case studies focused on

1) effects of wastewater treatment upgrades upstream of P8, and 2) effects of biological invasion on nutrient dynamics in Suisun Bay using observations from D7. Each case study is built around hypotheses that results from WRTDS models were expected to support, both as a general description and for additional testing with alternative methods.

### ***3.3.1 Effects of wastewater treatment***

Significant efforts have been made in recent years to reduce nitrogen loading from regional WWTPs given the disproportionate contribution of nutrients relative to other sources (Cornwell et al. 2014, Novick et al. 2015). Several WWTPs in the Delta have recently been or are planned to be upgraded to include tertiary filtration and nitrification to convert biologically available ammonium to nitrate. The City of Stockton WWTP was upgraded in 2006 and is immediately upstream of station P8 (Jabusch et al. 2016), which provides a valuable opportunity to assess how nutrient or nutrient-related source controls and water management actions have changed ambient concentrations downstream. A modal response of nutrient concentrations at P8 centered around 2006 is expected as a result of upstream WWTP upgrades, and water quality should exhibit 1) a shift in the ratio of the components of DIN from the WWTP before/after upgrade, and 2) a flow-normalized annual trend at P8 to show a change concurrent with WWTP upgrades.

Effluent measured from 2003 to 2009 from the Stockton WWTP had a gradual reduction in ammonium concentration relative to total DIN (Fig. 7). Ammonium and nitrate concentrations were comparable prior to 2006, whereas nitrate was a majority of total nitrogen after the upgrade, with much smaller percentages from ammonium and nitrite. As expected, flow-normalized nitrogen trends at P8 shifted in response to upstream WWTP upgrades (Fig. 8a), with ammonium showing an increase from 1976 followed by a large reduction in the 2000s. Interestingly, nitrite/nitrate concentrations also showed a similar but less dramatic decrease despite an increase

in the WWTP effluent concentrations following the upgrade. Percent changes from seasonal Kendall tests on flow-normalized results showed that both nitrogen species increased prior to WWTP upgrades (2% per year for nitrite/nitrate, 2.8% for ammonium), followed by decreases after upgrades (−1.9% for nitrite/nitrate, −16.6% for ammonium, Table 4). Seasonally, increases prior to upgrades were highest in the summer for nitrite/nitrate (2.4%) and in the fall for ammonium (4.9%). Similarly, seasonal reductions post-upgrade were largest in the summer for nitrite/nitrate (−4.3%) and largest for ammonium in the winter (−26.7%).

Relationships of nitrite/nitrate with flow described by WRTDS showed an inverse flow and concentration dynamic with flushing or dilution at higher flow (Fig. 8b). Seasonal variation was even more apparent for ammonium, although both nitrite/nitrate and ammonium typically had the highest concentrations at low flow in the winter (January). Additionally, strength of the flow/nutrient relationship changed between years. Nitrite/nitrate typically had the strongest relationship with flow later in the time series (i.e., larger negative slope), whereas ammonium had the strongest relationship with flow around 2000 in January.

### 3.3.2 *Effects of biological invasions*

Invasion of the upper SFE by the Asian clam *Potamocorbula amurensis* in 1986 caused severe changes in phytoplankton abundance and species composition. Reduction in phytoplankton biomass has altered trophic networks in the upper SFE and is considered an important mechanism in the decline of the protected delta smelt (*Hypomesus transpacificus*) and other important fisheries (Feyrer et al. 2003, Mac Nally et al. 2010). Changes in the physical environment have also occurred, particularly increased water clarity from a reduction of particle transport and erodible sediment supply (Jassby 2008, Schoellhamer 2011, Cloern and Jassby 2012), although decreases in phytoplankton by clam biofiltration may have also increased clarity

(Mac Nally et al. 2010). The clams are halophilic such that drought years are correlated with an increase in biomass and further upstream invasion of the species (Parchaso and Thompson 2002, Cloern and Jassby 2012). We hypothesized that results from WRTDS models would show 1) a decline in annual, flow-normalized chlorophyll concentrations over time coincident with an increase in abundance of invaders, and 2) variation in the chlorophyll/clam relationship through indirect or direct controls of flow. Although the relationship between phytoplankton and clams have been well described in SFE (Kimmerer and Thompson 2014), we use WRTDS to develop additional evidence that an increase in DIN was facilitated in part by clam invasion.

Invasion in the 1980s showed a clear reduction of *Corbicula fluminea* and increase of *P. amurensis* (Fig. 9a), where biomass of the latter was negatively associated with flow from the Sacramento river (Fig. 9b). The increase in clam abundance was associated with a notable decrease in annually-averaged chl-*a* from WRTDS results (Fig. 9c), as expected if WRTDS is adequately capturing flow variation and identifying the well-established phytoplankton decrease beginning in the 1980s. A seasonal shift in the flow-normalized results was also observed such that chl-*a* concentrations were generally highest in July/August prior to invasion, whereas a spring maximum in April was more common in recent years (Fig. 9f). An increase in annually-averaged silicon dioxide (Fig. 9e) was coincident with the chl-*a* decrease, with the largest increases occurring in August (Fig. 9g). These relationships suggest that diatoms were the dominant genera early in the time series, particularly in late summer, whereas the spring peak observed in later years represents a shift to an earlier seasonal maxima. This supports past research that showed a decrease in silica uptake by diatoms following invasion (Cloern 1996, Kimmerer 2005). Further, DIN trends were similar to silicon-dioxide in both annual and seasonal changes (i.e., Figures 9e and 9h compared to 9d and 9g), such that an increase in both nutrients



earlier in the time series corresponded with the decrease in chl-*a*. Overall, these results suggest that a nontrivial portion of the DIN increase could be related to the decrease in a major ‘sink’, i.e., decreased DIN uptake by phytoplankton due to top down grazing pressure from *P. amurensis*.

The relationship of chl-*a* with clam biomass was significant (Fig. 9i), with lower chl-*a* associated with higher biomass, confirming results from earlier studies (Alpine and Cloern 1992, Thompson et al. 2008). However, the effect of flow on both clams and phytoplankton as a top-down or bottom-up control changed throughout the time series. The chl-*a*/flow relationship showed that increasing flow (decreasing salinity) was associated with a slight increase in chl-*a* followed by a decrease early in the time series (Fig. 9j), whereas overall chl-*a* was lower but a positive association with flow (negative with salinity) was observed later in the time series. In the absence of benthic grazing prior to invasion, this dynamic suggests that chl-*a* production may be limited at low flow as less nutrients are exported from the Delta, stimulated as flow increases, and reduced at high flow as either nutrients or phytoplankton biomass are exported to the larger bay. Following clam invasion, chl-*a* concentrations were reduced by grazing but showed a positive and monotonic relationship with increasing flow. The increase in clam abundance was concurrent with decline in chl-*a* concentration, although variation in abundance between years was also observed. Clam abundance was reduced during high flow years in the late 1990s, 2006, and 2011 (9a). In the same years, WRTDS predictions for chl-*a* were higher than the flow-normalized component (Fig. 9c), which further suggests a link between increased flow and phytoplankton production.

## 4 Discussion

Differences in apparent trends underscore the importance of considering flow effects in the interpretation of environmental changes, particularly if trend evaluation is used to assess the

effects of nutrients on ecosystem health or the effectiveness of past nutrient management actions. Our results demonstrated the potential to misinterpret trends if flow effects are not considered, where the misinterpretation could vary from a simple change in the magnitude and significance of a trend, to more problematic changes where the flow-normalized trend could demonstrate a complete reversal relative to the observed (e.g., DIN trends for all Suisun stations from 1996-2013, Fig. 4). A more comprehensive evaluation of flow in the Delta demonstrated that flow contributions of different end members vary considerably over time at each station (Novick et al. 2015). For example, flow at MD10 represents a changing percentage by season of inputs from the Sacramento, San Joaquin, Cosumnes, Mokelumne rivers, and agricultural returns. For simplicity, water quality observations in our analyses were matched with large-scale drivers of flow into the Delta where most sites were matched to Sacramento or San Joaquin daily flow estimates. Given that substantial differences with flow-normalized results were apparent from relatively coarse estimates of flow contributions, more precise differences could be obtained by considering the influence of multiple flow components at each location. Output from the Dayflow software program (IEP 2016) provides a complete mass balance of flow in the Delta that could be used to develop a more comprehensive description.

A general conclusion is that ammonium reductions were concurrent with WWTP upgrades, but the reduction was most apparent at low-flow in January. These dynamics are difficult to characterize from the observed time series, and further, results from WRTDS can be used to develop additional hypotheses of factors that influence nutrient concentrations at P8. For example, estimated ammonium concentrations in July were low for all flow levels which suggests either nitrogen inputs were low in the summer or nitrogen was available and uptake by primary consumers was high. Seasonal patterns in the relationship between flow and nitrite/nitrate were

not as dramatic as compared to ammonium, and in particular, low-flow events in July were associated with higher concentrations. This could suggest that ammonium concentrations at P8 are driving phytoplankton production at low flow during warmer months, and not nitrite/nitrate given the higher estimated concentrations in July at low flow. As such, these simple observations provide quantitative support of cause and effect mechanisms of nutrient impacts on potentially adverse environmental conditions as they relate to nutrient-related source controls upstream.

As such, chl-*a* production in early years is directly related to flow, whereas the relationship with flow in later years is indirect as increased flow reduces clam abundance and releases phytoplankton from benthic grazing pressure. These relationships have been suggested by others ([Alpine and Cloern 1992](#), [Parchaso and Thompson 2002](#), [Jassby 2008](#)), although the precise mechanism demonstrated by WRTDS provides a quantitative description of factors that drive water quality in the Delta.

As demonstrated by both case studies and the overall trends across all stations, water quality dynamics in the Delta are complex and driven by multiple factors that change through space and time. At a minimum, WRTDS provides a description of change by focusing on high-level forcing factors that explicitly account for annual, seasonal, and flow effects on trend interpretations. We have demonstrated the potential for imprecise or inaccurate conclusions of trend tests that focus solely on observed data and emphasize that flow-normalized trends have more power to quantify change. Moreover, trends in nutrient loads from point sources in the Delta have previously been described, e.g., Sacramento WWTP increases ([Jassby 2008](#)) and exports to Suisun Bay ([Novick and Senn 2014](#)). The results from WRTDS demonstrating these changes are not unexpected, and consequently, we are not detracting from the potential implications of such increases. The important conclusion is that the physical/hydrological and biogeochemical factors

that influence nutrient cycling and ambient concentrations in the Bay-Delta, and changes to those factors, are substantial enough that they can be comparable in magnitude to anthropogenic load increases or comparable to the effects of management actions to decrease nutrient levels. Therefore, methods that adjust for the effects of these factors are critical when studying long-term records to assess the impacts or effectiveness of load increases or management actions, respectively.

Combined with additional data, WRTDS results can support hypotheses that lead to a more comprehensive understanding of ecosystem dynamics. Additional factors to consider include the effects of large-scale climatic patterns, more detailed hydrologic descriptions, and additional ecological components that affect trophic interactions. For example, a more rigorous matching of flow time series with water quality observations at each station that considers varying source contributions over time could provide a more robust description of flow-normalized results. Alternative methods for time series analysis could also be used to address a wider range of questions, particularly those with more generic structural forms that can explicitly include additional variables (e.g., generalized additive models, [Beck and Murphy \(2017\)](#)). Overall, statistical interpretations of multiple factors can provide a basis for quantitative links between nutrient loads and adverse effects on ecosystem conditions, including the identification of thresholds for the protection and restoration of water quality.

## ***Acknowledgments***

We thank the staff of the San Francisco Estuary Institute and the Delta Regional Monitoring Program. We thank Larry Harding for providing comments on an earlier draft. This study was reviewed and approved for publication by the US EPA, National Health and

Environmental Effects Research Laboratory. The authors declare no competing financial interest.

The views expressed in this paper are those of the authors and do not necessarily reflect the views or policies of the US EPA.

## *References*

- Alpine AE, Cloern JE. 1988. Phytoplankton growth rates in a light-limited environment, San Francisco Bay. *Marine Ecology Progress Series*, 44(2):167–173.
- Alpine AE, Cloern JE. 1992. Trophic interactions and direct physical effects control phytoplankton biomass and production in an estuary. *Limnology and Oceanography*, 37(5):946–955.
- Beck MW. 2017. WRTDStidal: Weighted Regression for Water Quality Evaluation in Tidal Waters. R package version 1.1.0.
- Beck MW, Hagy III JD. 2015. Adaptation of a weighted regression approach to evaluate water quality trends in an estuary. *Environmental Modelling and Assessment*, 20(6):637–655.
- Beck MW, Murphy RR. 2017. Numerical and qualitative contrasts of two statistical models for water quality change in tidal waters. *Journal of the American Water Resources Association*, 53(1):197–219.
- Canuel EA, Lerberg EJ, Dickhut RM, Kuehl SA, Bianchi TS, Wakeham SG. 2009. Changes in sediment and organic carbon accumulation in a highly-disturbed ecosystem: The Sacramento-San Joaquin River Delta (California, USA). *Marine Pollution Bulletin*, 59(4-7):154–163.
- Cloern JE. 1996. Phytoplankton bloom dynamics in coastal ecosystems: A review with some general lessons from sustained investigation of San Francisco Bay, California. *Review of Geophysics*, 34(2):127–168.
- Cloern JE. 2015. Life on the edge: California’s estuaries. In: Mooney H, Zavaleta E, editors, *Ecosystems of California: A Source Book*, pages 359–387. University of California Press, California.
- Cloern JE, Jassby AD. 2010. Patterns and scales of phytoplankton variability in estuarine-coastal ecosystems. *Estuaries and Coasts*, 33(2):230–241.
- Cloern JE, Jassby AD. 2012. Drivers of change in estuarine-coastal ecosystems: Discoveries from four decades of study in San Francisco Bay. *Reviews of Geophysics*, 50(4):1–33.
- Cloern JE, Jassby AD, Thompson JK, Hieb KA. 2007. A cold phase of the East Pacific triggers new phytoplankton blooms in San Francisco Bay. *Proceedings of the National Academy of Sciences of the United States of America*, 104(47):18561–18565.

- Cloern JE, Schraga TS, Lopez CB, Knowles N, Labiosa RG, Dugdale R. 2005. Climate anomalies generate an exceptional dinoflagellate bloom in San Francisco Bay. *Geophysical Research Letters*, 32(14):L14608.
- Cohen AN, Carlton JT. 1998. Accelerating invasion rate in a highly invaded estuary. *Science*, 279(5350):555–558.
- Cole BE, Cloern JE. 1984. Significance of biomass and light availability to phytoplankton productivity in San Francisco Bay. *Marine Ecology Progress Series*, 17(1):15–24.
- Cornwell JC, Glibert PM, Owens MS. 2014. Nutrient fluxes from sediments in the San Francisco Bay Delta. *Estuaries and Coasts*, 37(5):1120–1133.
- Crauder JS, Thompson JK, Parchaso F, Anduaga RI, Pearson SA, Gehrts K, Fuller H, Wells E. 2016. Bivalve effects on the food web supporting delta smelt - a long-term study of bivalve recruitment, biomass, and grazing rate patterns with varying freshwater outflow. Technical Report Open-File Report 2016-1005, US Geological Survey, Reston, Virginia.
- Dortch W. 1990. The interaction between ammonium and nitrate uptake in phytoplankton. *Marine Ecology Progress Series*, 61(1/2):183–201.
- Dugdale RC, Wilkerson FP, Hogue VE, Marchi A. 2007. The role of ammonium and nitrate in spring bloom development in San Francisco Bay. *Estuarine, Coastal, and Shelf Science*, 73:17–29.
- Enright C, Culbertson SD. 2009. Salinity trends, variability, and control in the northern reach of the San Francisco Estuary. *San Francisco Estuary and Watershed Science*, 7(2):1–28.
- Feyrer F, Herbold B, Matern SA, Moyle PB. 2003. Dietary shifts in a stressed fish assemblage: Consequences of a bivalve invasion in the San Francisco Estuary. *Environmental Biology of Fishes*, 67(3):277–288.
- Glibert PM, Dugdale RC, Wilkerson F, Parker AE, Alexander J, Antell E, Blaser S, Johnson A, Lee J, Lee T, Murasko S, Strong S. 2014. Major - but rare - spring blooms in san francisco bay delta, california, a result of long-term drought, increased residence time, and altered nutrient loads and forms. *Journal of Experimental Marine Biology and Ecology*, 460:8–18.
- Harding LW, Gallegos CL, Perry ES, Miller WD, Adolf JE, Mallonee ME, Paerl HW. 2016. Long-term trends of nutrients and phytoplankton in Chesapeake Bay. *Estuaries and Coasts*, 39:664–681.
- Hirsch RM, De Cicco L. 2014. User guide to Exploration and Graphics for RivEr Trends (EGRET) and dataRetrieval: R packages for hydrologic data. Technical Report Techniques and Methods book 4, ch. A10, US Geological Survey, Reston, Virginia.  
<http://pubs.usgs.gov/tm/04/a10/>.
- Hirsch RM, Moyer DL, Archfield SA. 2010. Weighted regressions on time, discharge, and season (WRTDS), with an application to Chesapeake Bay river inputs. *Journal of the American Water Resources Association*, 46(5):857–880.

- Hirsch RM, Slack JR, Smith RA. 1982. Techniques of trend analysis for monthly water quality data. *Water Resources Research*, 18:107–121.
- IEP. 2013. IEP Bay-Delta Monitoring and Analysis Section, Discrete Water Quality Metadata. <http://water.ca.gov/bdma/meta/discrete.cfm>.
- IEP. 2016. Dayflow: An estimate of daily average Delta outflow. Interagency Ecological Program for the San Francisco Estuary. <http://www.water.ca.gov/dayflow/>.
- Jabusch T, Bresnahan P, Trowbridge P, Novick E, Wong A, Salomon M, Senn D. 2016. Summary and evaluation of Delta subregions for nutrient monitoring and assessment. Technical report, San Francisco Estuary Institute, Richmond, CA.
- Jabusch T, Gilbreath AN. 2009. Summary of current water quality monitoring programs in the Delta. Technical report, San Francisco Estuary Institute, Richmond, CA.
- Jassby AD. 2008. Phytoplankton in the Upper San Francisco Estuary: Recent biomass trends, their causes, and their trophic significance. *San Francisco Estuary and Watershed Science*, 6(1):1–24.
- Jassby AD, Cloern JE. 2000. Organic matter sources and rehabilitations of the Sacramento-San Joaquin Delta (California, USA). *Aquatic Conservation: Marine and Freshwater Ecosystems*, 10:323–352.
- Jassby AD, Cloern JE, Cole BE. 2002. Annual primary production: Patterns and mechanisms of change in a nutrient-rich tidal ecosystem. *Limnology and Oceanography*, 47(3):698–712.
- Kimmerer W. 2005. Long-term changes in apparent uptake of silica in the San Francisco Estuary. *Limnology and Oceanography*, 50(3):793–798.
- Kimmerer WJ, Parker AE, Lidstrom UE, Carpenter EJ. 2012. Short-term and interannual variability in primary production in the low-salinity zone of the San Francisco Estuary. *Estuaries and Coasts*, 35:913–929.
- Kimmerer WJ, Thompson JK. 2014. Phytoplankton growth balanced by clam and zooplankton grazing and net transport into the low-salinity zone of the San Francisco Estuary. *Estuaries and Coasts*, 37:1202–1218.
- Lehman PW. 2000. The influence of climate on phytoplankton community biomass in San Francisco Bay Estuary. *Limnology and Oceanography*, 45(3):580–590.
- Lehman PW, Boyer G, Hall C, Waller S, Gehrts K. 2005. Distribution and toxicity of a new colonial *Microcystis aeruginosa* bloom in the San Francisco Bay Estuary, California. *Hydrobiologia*, 541:87–99.
- Lehman PW, Teh SJ, Boyer GL, Nobriga ML, Bass E, Hogle C. 2010. Initial impacts of *Microcystis aeruginosa* blooms on the aquatic food web in the San Francisco Estuary. *Hydrobiologia*, 637(1):229–248.

- Levin SA. 1992. The problem of pattern and scale in ecology. *Ecology*, 73(6):1943–1967.
- Mac Nally R, Thompson JR, Kimmerer WJ, Feyrer F, Newman KB, Sih A, Bennett WA, Brown L, Fleishman E, Culberson SD, Castillo G. 2010. Analysis of pelagic species decline in the upper San Francisco Estuary using multivariate autoregressive modeling (MAR). *Ecological Applications*, 20(5):1417–1430.
- Medalie L, Hirsch RM, Archfield SA. 2012. Use of flow-normalization to evaluate nutrient concentration and flux changes in Lake Champlain tributaries, 1990-2009. *Journal of Great Lakes Research*, 38(SI):58–67.
- Millard SP. 2013. *EnvStats: An R Package for Environmental Statistics*. Springer, New York.
- Nichols FH. 1985. Increased benthic grazing: An alternative explanation for low phytoplankton biomass in northern San Francisco Bay during the 1976-1977 drought. *Estuarine, Coastal and Shelf Science*, 21(3):379–388.
- Novick E, Holleman R, Jabusch T, Sun J, Trowbridge P, Senn D, Guerin M, Kendall C, Young M, Peek S. 2015. Characterizing and quantifying nutrient sources, sinks and transformations in the Delta: synthesis, modeling, and recommendations for monitoring. Technical Report Contribution Number 785, San Francisco Estuary Institute, Richmond, CA.
- Novick E, Senn D. 2014. External nutrient loads to San Francisco Bay. Technical Report Contribution Number 704, San Francisco Estuary Institute, Richmond, CA.
- O'Neill RV, Johnson AR, King AW. 1989. A hierarchical framework for the analysis of scale. *Landscape Ecology*, 3(3-4):193–205.
- Parchaso F, Thompson JK. 2002. Influence of hydrologic processes on reproduction of the introduced bivalve *Potamocorbula amurensis* in northern San Francisco Bay, California. *Pacific Science*, 56(3):329–345.
- Pellerin BA, Bergamaschi BA, Gilliom RJ, Crawford CG, Saraceno JF, Frederick CP, Downing BD, Murphy JC. 2014. Mississippi River nitrate loads from high frequency sensor measurements and regression-based load estimation. *Environmental Science and Technology*, 48:12612–12619.
- RDCT (R Development Core Team). 2017. *R: A language and environment for statistical computing*, v3.3.2. R Foundation for Statistical Computing, Vienna, Austria.  
<http://www.R-project.org>.
- Sakamoto M, Tanaka T. 1989. Phosphorus dynamics associated with phytoplankton blooms in eutrophic Mikawa Bay, Japan. *Marine Biology*, 101(2):265–271.
- Schoellhamer DH. 2011. Sudden clearing of estuarine waters upon crossing the threshold from transport to supply regulation of sediment transport as an erodible sediment pool is depleted: San Francisco bay, 1999. *Estuaries and Coasts*, 34:885–899.



- Schultz P, Urban NR. 2008. Effects of bacterial dynamics on organic matter decomposition and nutrient release from sediments: A modeling study. *Ecological Modelling*, 210(1-2):1–14.
- Shellenbarger GG, Schoellhamer DH, Morgan TL, Takekawa JY, Athearn ND, Henderson KD. 2008. Dissolved oxygen in Guadalupe Slough and Pond A3W, South San Francisco Bay, California, August and September 2007. Technical Report Open-File Report 2008-1097, US Geological Survey, Reston, Virginia.
- Sprague LA, Hirsch RM, Aulenbach BT. 2011. Nitrate in the Mississippi River and its tributaries, 1980 to 2008: Are we making progress? *Environmental Science and Technology*, 45(17):7209–7216.
- Sutula M, Kudela R, III JDH, Jr. LWH, Senn D, Cloern JE, Bricker S, Berg GM, Beck MW. 2017. Novel analyses of long-term data provide a scientific basis for chlorophyll-a thresholds in San Francisco Bay. *Estuarine, Coastal and Shelf Science*, 197:107–118.
- Thompson JK, Koseff JR, Monismith SG, Lucas LV. 2008. Shallow water processes govern system-wide phytoplankton bloom dynamics: A field study. *Journal of Marine Systems*, 74(1-2):153–166.
- Tobin J. 1958. Estimation of relationships for limited dependent variables. *Econometrica*, 26(1):24–36.
- Wright SA, Schoellhamer DH. 2004. Trends in the sediment yield of the Sacramento River, California, 1957-2001. *San Francisco Estuary and Watershed Science*, 2(2):1–14.
- Zhang Q, Harman CJ, Ball WP. 2016. An improved method for interpretation of riverine concentration-discharge relationships indicates long-term shifts in reservoir sediment trapping. *Geophysical Research Letters*, 43(10):215–224.

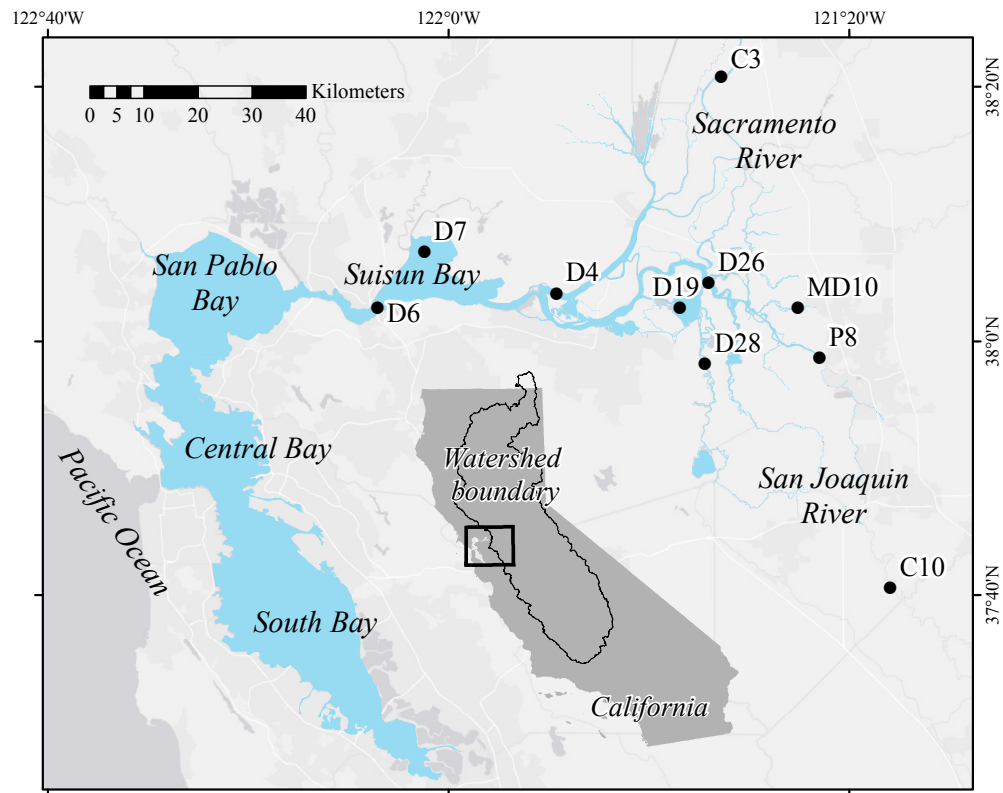


Fig. 1: The San Francisco Estuary and Delta region with monitoring stations used for analysis. The Delta drains the combined watersheds of the Sacramento and San Joaquin rivers (inset). All data were obtained from the Interagency Ecological Program website (<http://water.ca.gov/bdma/meta/Discrete/data.cfm>, IEP (2013)).

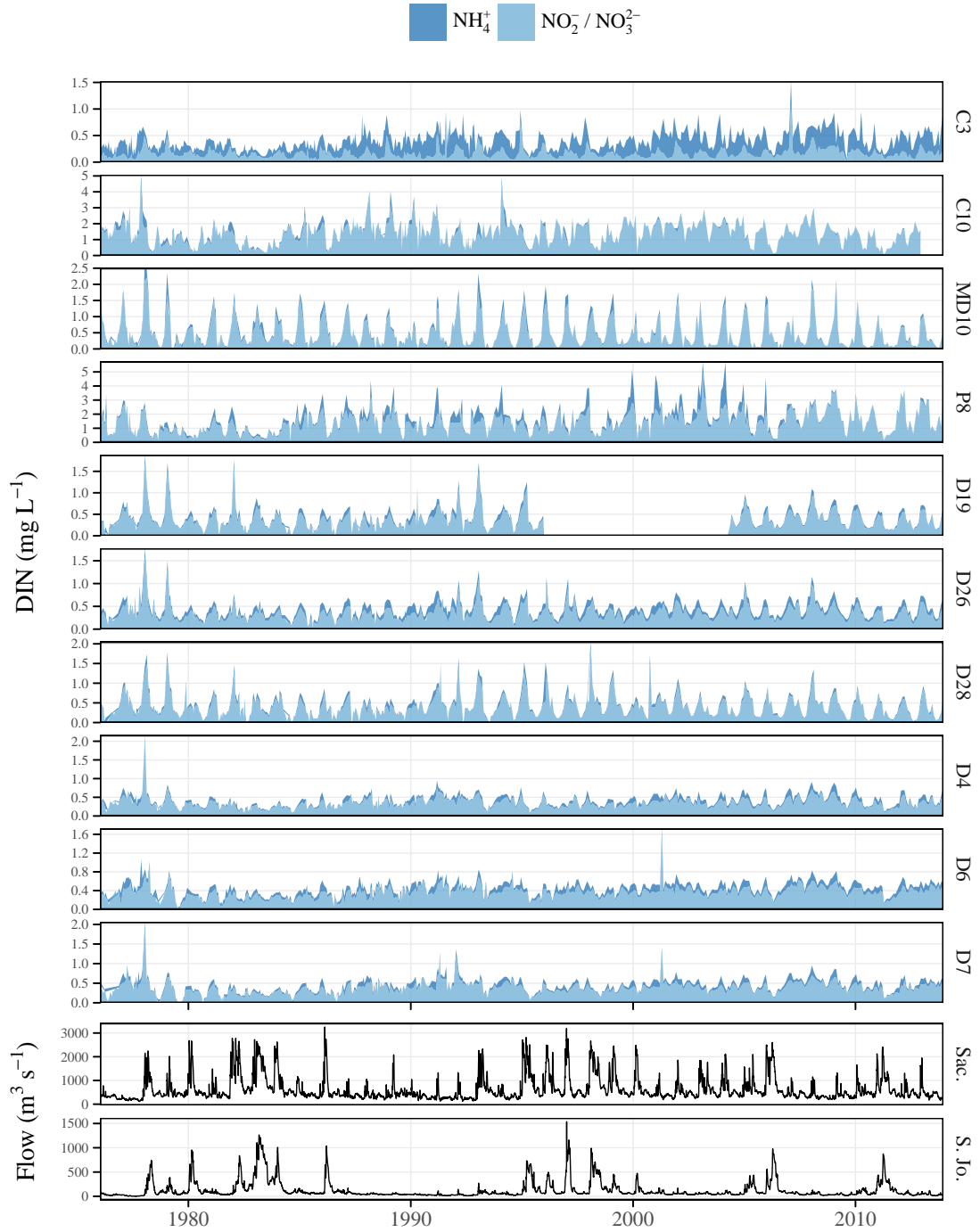


Fig. 2: Observed DIN ( $\text{NH}_4^+ + \text{NO}_2^-/\text{NO}_3^{2-}$ ) from ten stations in the upper SFE Delta and flow from the Sacramento and San Joaquin rivers. Data were collected monthly and evaluated with WRTDS models using daily flow estimates from 1976 to 2013. Note different y-axis scales. See Fig. 1 for station locations.

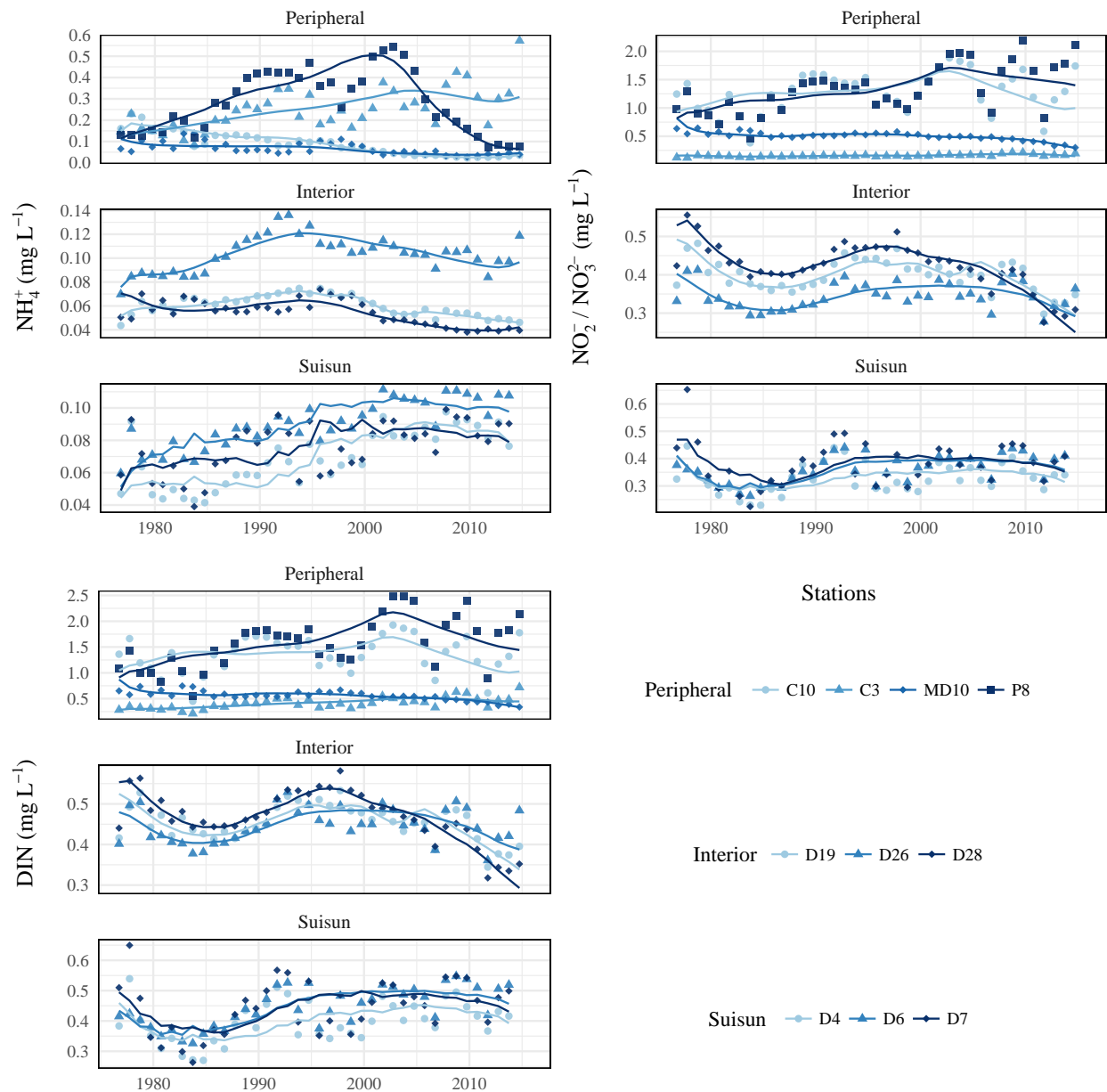


Fig. 3: Model predictions for ten stations grouped by nitrogen analyte and geographic location in the Delta region (locations in Fig. 1). Results are annually-averaged for each water year from October to September. Points are model predictions and lines are flow-normalized predictions.

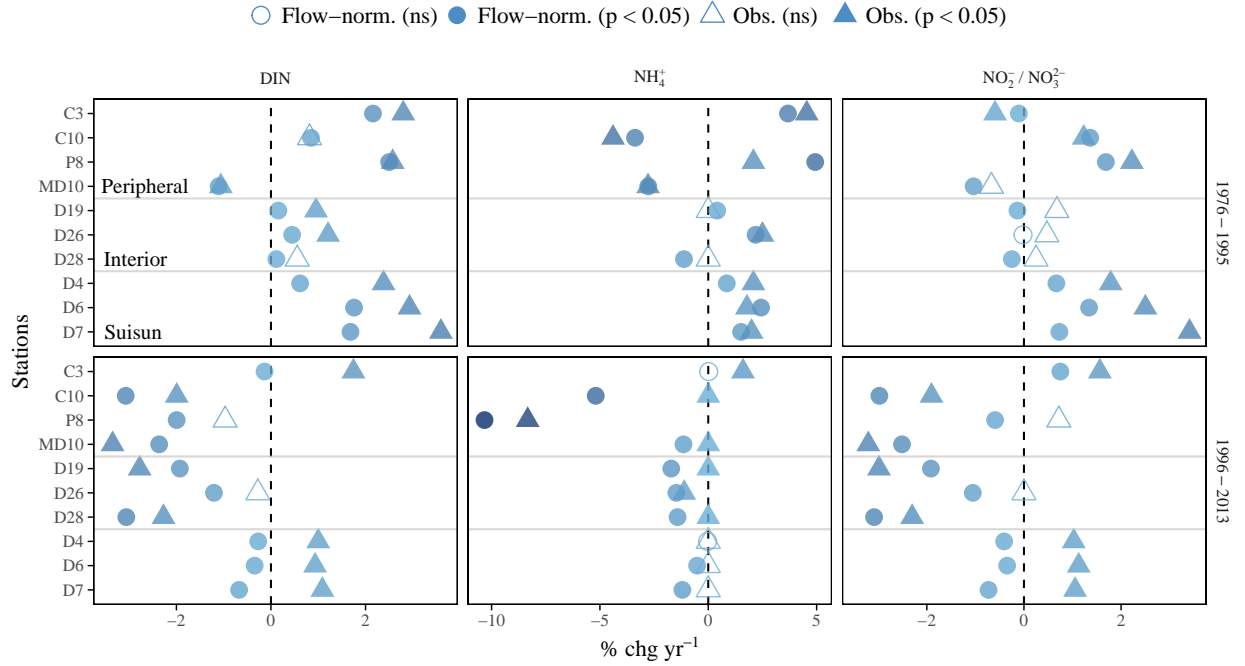


Fig. 4: Results from seasonal Kendall tests on observed data (triangles) and flow-normalized predictions (circles) from WRTDS for nitrogen analytes. Results are shown as the percent change per year as the estimated Theil-Sen slope divided by the median for a given aggregation period (significance evaluated at  $\alpha = 0.05$ , based on  $\tau$ ). Trends are shown separately for different annual groupings. See Figs. 5 and 6 for seasonal groupings.

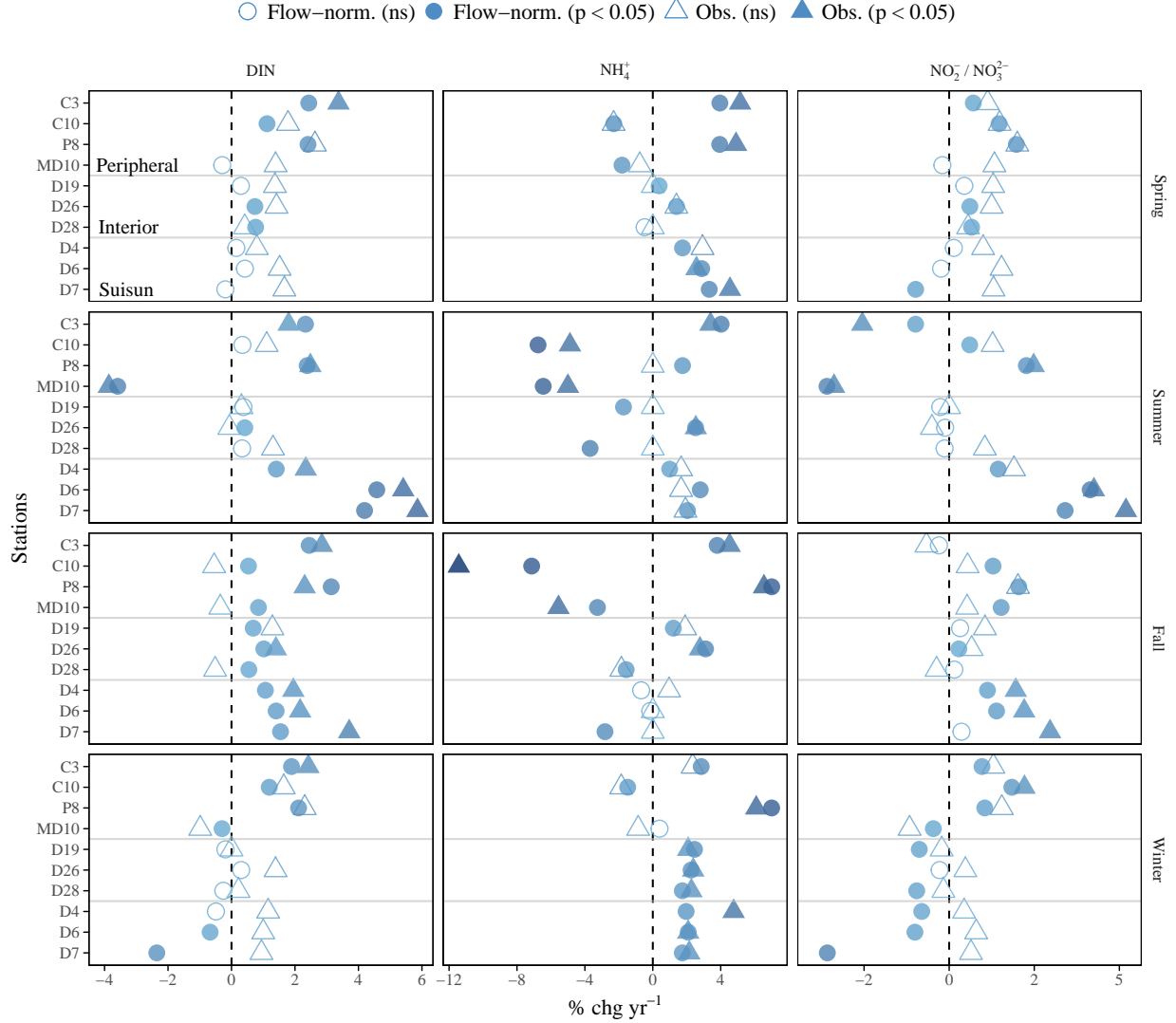


Fig. 5: Results from seasonal Kendall tests on observed data (triangles) and flow-normalized predictions (circles) from WRTDS for nitrogen analytes. Results are shown as the percent change per year as the estimated Theil-Sen slope divided by the median for a given aggregation period (significance evaluated at  $\alpha = 0.05$ , based on  $\tau$ ). Trends are shown separately for different seasonal groupings from 1976-1995. Months for each season are Spring: MAM, Summer: JJA, Fall: SON, Winter: DJF. See Figure 3 for annual comparisons.

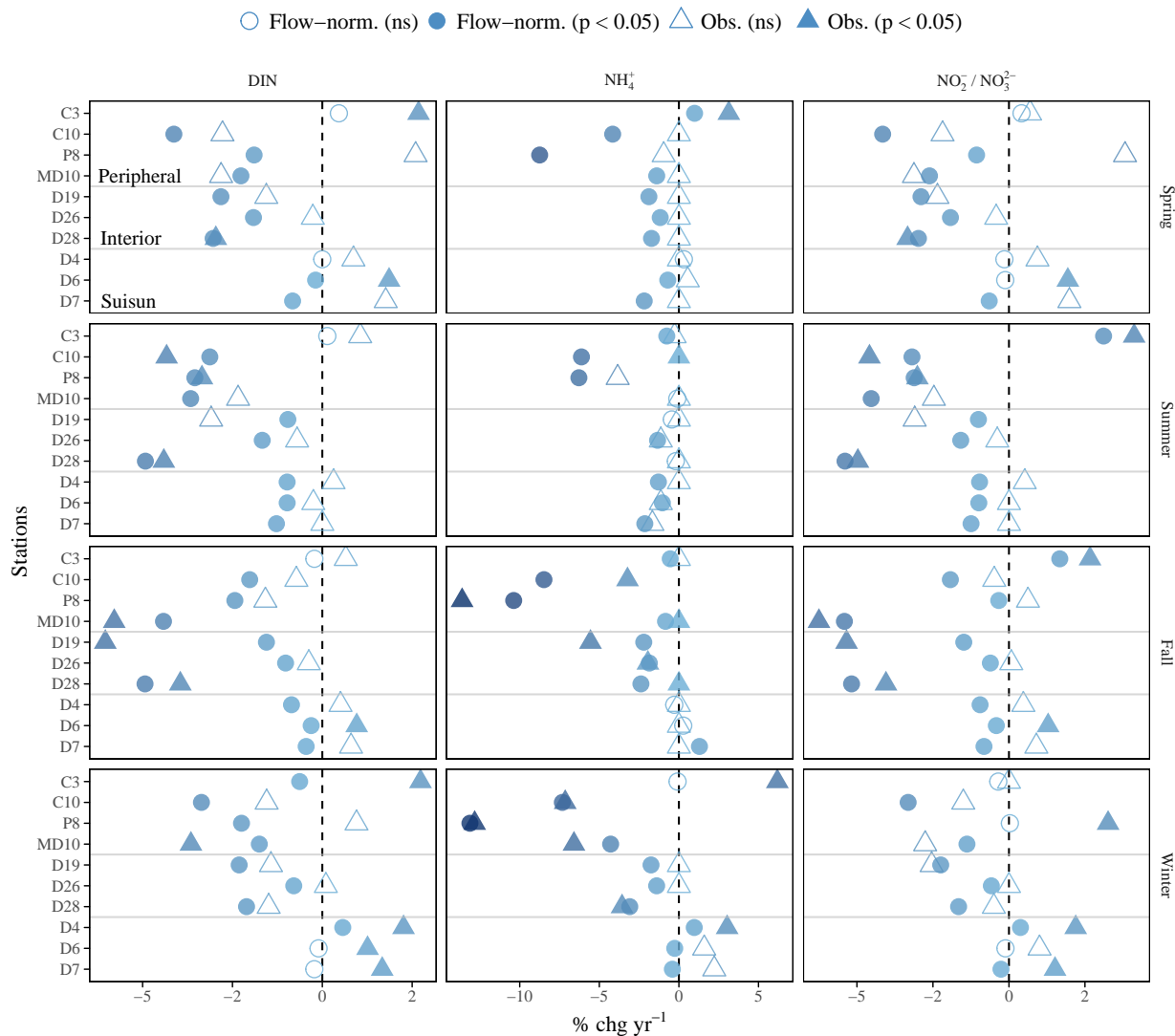


Fig. 6: Results from seasonal Kendall tests on observed data (triangles) and flow-normalized predictions (circles) from WRTDS for nitrogen analytes. Results are shown as the percent change per year as the estimated Theil-Sen slope divided by the median for a given aggregation period (significance evaluated at  $\alpha = 0.05$ , based on  $\tau$ ). Trends are shown separately for different seasonal groupings from 1996-2013. Months for each season are Spring: MAM, Summer: JJA, Fall: SON, Winter: DJF. See Figure 3 for annual comparisons.

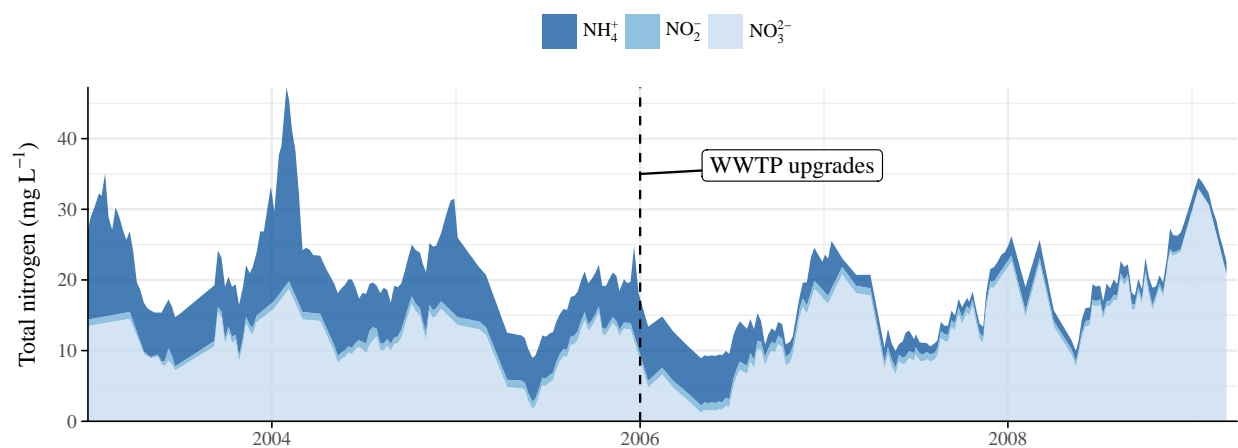


Fig. 7: Nitrogen concentration measurements ( $\text{mg L}^{-1}$ ) from the City of Stockton Wastewater Treatment Plant, San Joaquin County. Wastewater discharge requirements were implemented in 2006 for nitrification/denitrification and tertiary filtration to convert ammonium to nitrate.



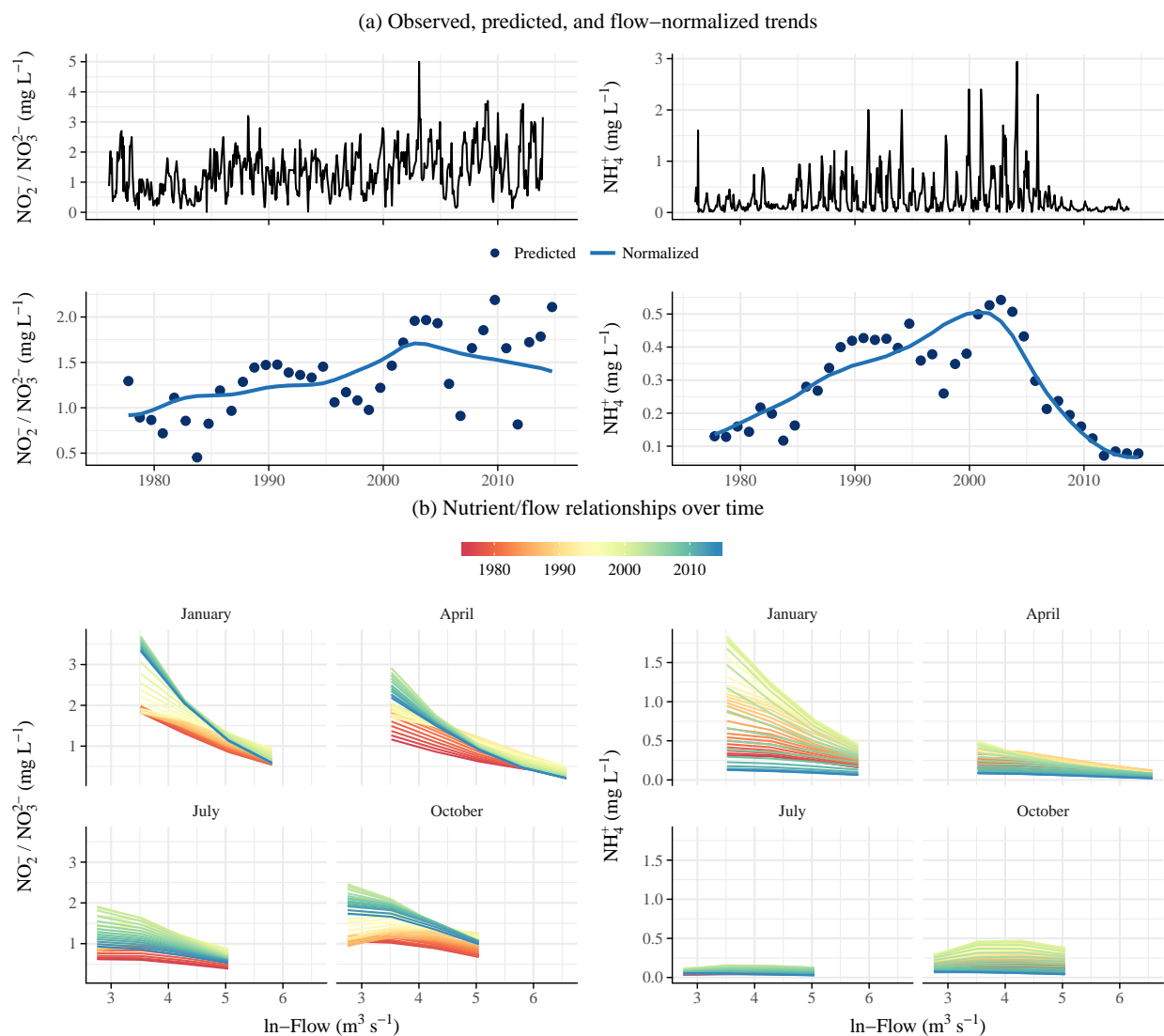


Fig. 8: Nitrogen trends at P8 as (a, top) observed, (a, bottom) predicted and flow-normalized estimates from WRTDS, and (b) relationships with flow over time from WRTDS. Nitrite/nitrate trends are on the left and ammonium trends are on the right. Wastewater treatment plant upgrades at the City of Stockton (San Joaquin County) were completed in 2006 (Fig. 7).

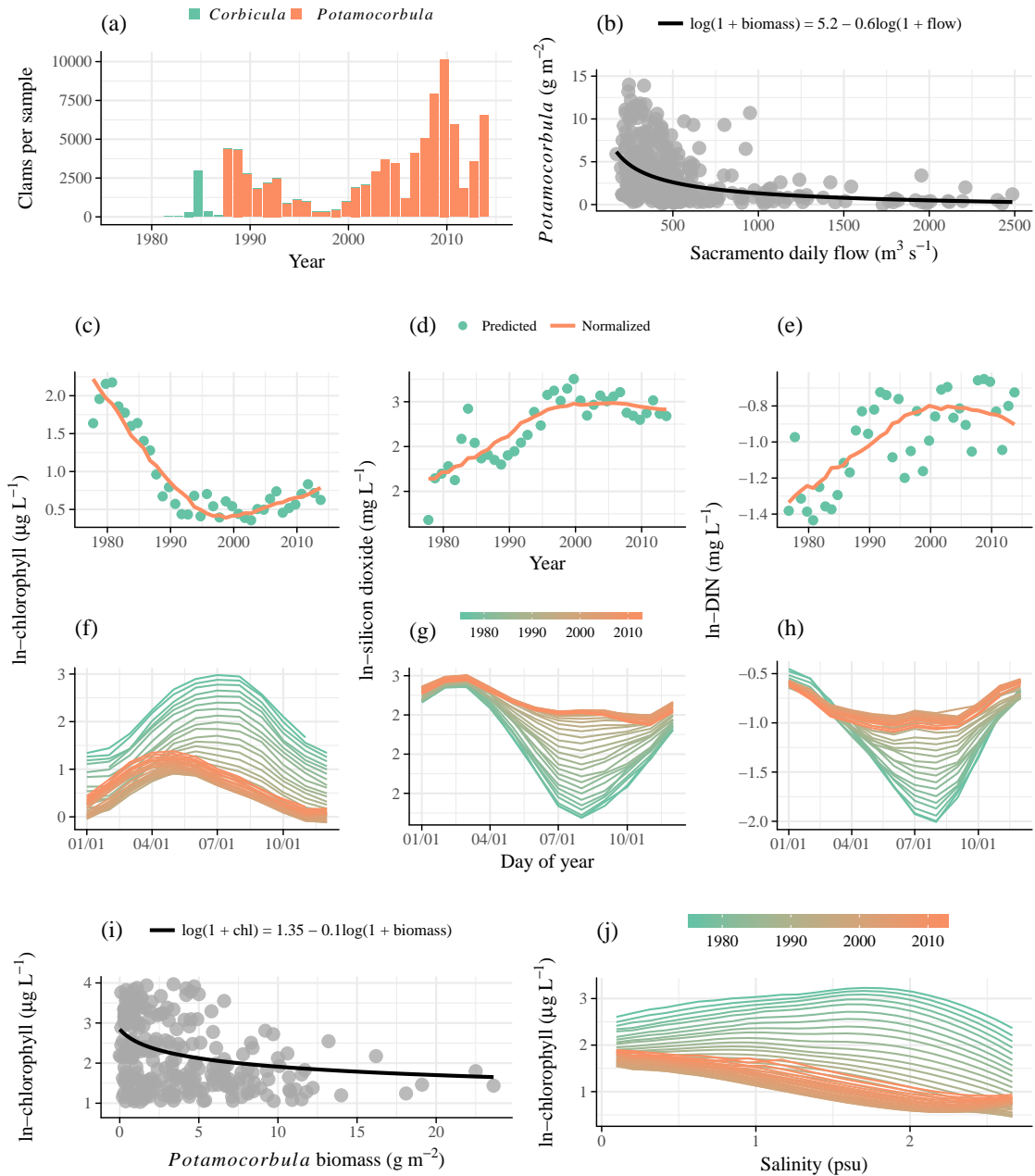


Fig. 9: Trends in clam abundance and chl-*a* concentration from 1976 to 2013 at station D7 in Suisun Bay. Invasion by *Potamocorbula amurensis* clams in the late 1980s and reduction of *Corbicula fluminea* was shown by changes in clam density (a, annual means), with biomass linked to salinity (b). A decrease in chl-*a* concentration was also observed by changes in annual (c) and seasonal trends (f) based on WRTDS results. Reductions in chl-*a* concentration were coincident with an increase in  $\text{SiO}_2$  and DIN concentrations (d, e), with the greatest increases in August (g, h). A significant ( $p < 0.001$ ) relationship between clam biomass and chl-*a* concentration is shown in subfigure (i). Flow relationships with chl-*a* concentration shown by WRTDS have also changed over time (j, observations from June).

Table 1: Summaries of flow-normalized trends in nitrogen analytes for all stations and annual aggregations

Analyte/Station	Annual	
	1976-1995	1996-2013
<b>DIN</b>		
C10	1.3 ( <b>0.8</b> )**	1.4 (-3.1)**
C3	0.3 ( <b>2.2</b> )**	0.5 (-0.1)**
D19	0.4 ( <b>0.2</b> )**	0.4 (-1.9)**
D26	0.4 ( <b>0.4</b> )**	0.5 (-1.2)**
D28	0.4 ( <b>0.1</b> )**	0.4 (-3.1)**
D4	0.3 ( <b>0.6</b> )**	0.4 (-0.3)**
D6	0.4 ( <b>1.8</b> )**	0.5 (-0.3)**
D7	0.4 ( <b>1.7</b> )**	0.5 (-0.7)**
MD10	0.4 (-1.1)**	0.3 (-2.4)**
P8	1.3 ( <b>2.5</b> )**	1.7 (-2)**
<b>NH<sub>4</sub><sup>+</sup></b>		
C10	0.1 (-3.4)**	0 (-5.2)**
C3	0.2 ( <b>3.7</b> )**	0.3 ( <b>0</b> )
D19	0 ( <b>0.4</b> )**	0 (-1.7)**
D26	0.1 ( <b>2.2</b> )**	0.1 (-1.5)**
D28	0 (-1.1)**	0 (-1.4)**
D4	0 ( <b>0.9</b> )**	0.1 ( <b>0</b> )
D6	0.1 ( <b>2.4</b> )**	0.1 (-0.5)**
D7	0.1 ( <b>1.5</b> )**	0.1 (-1.2)**
MD10	0.1 (-2.8)**	0 (-1.1)**
P8	0.2 ( <b>4.9</b> )**	0.1 (-10.3)**
<b>NO<sub>2</sub><sup>-</sup>/NO<sub>3</sub><sup>2-</sup></b>		
C10	1.2 ( <b>1.4</b> )**	1.4 (-3)**
C3	0.1 (-0.1)**	0.2 ( <b>0.7</b> )**
D19	0.4 (-0.1)**	0.4 (-1.9)**
D26	0.3 ( <b>0</b> )	0.4 (-1.1)**
D28	0.4 (-0.2)**	0.4 (-3.1)**
D4	0.3 ( <b>0.7</b> )**	0.3 (-0.4)**
D6	0.3 ( <b>1.3</b> )**	0.4 (-0.3)**
D7	0.4 ( <b>0.7</b> )**	0.4 (-0.7)**
MD10	0.4 (-1)**	0.3 (-2.5)**
P8	1.2 ( <b>1.7</b> )**	1.5 (-0.6)**

Summaries are medians (mg L<sup>-1</sup>) and percent change per year in parentheses (increasing in bold-italic). Changes and significance estimates are based on seasonal Kendall tests of flow-normalized results within each time period.  
 \* $p < 0.05$ ; \*\* $p < 0.005$

Table 2: Summaries of flow-normalized trends in nitrogen analytes for all stations and seasonal aggregations from 1976-1995

Analyte/Station	Seasonal, 1976-1995			
	Spring	Summer	Fall	Winter
<b>DIN</b>				
C10	1.2 ( <i>1.1</i> )**	1.2 ( <i>0.3</i> )	1.3 ( <i>0.5</i> )**	1.7 ( <i>1.2</i> )**
C3	0.3 ( <i>2.4</i> )**	0.3 ( <i>2.3</i> )**	0.4 ( <i>2.4</i> )**	0.4 ( <i>1.9</i> )**
D19	0.5 ( <i>0.3</i> )	0.2 ( <i>0.4</i> )	0.3 ( <i>0.7</i> )**	0.7 (-0.2)
D26	0.4 ( <i>0.7</i> )**	0.3 ( <i>0.4</i> )*	0.4 ( <i>1</i> )**	0.6 ( <i>0.3</i> )
D28	0.5 ( <i>0.8</i> )*	0.2 ( <i>0.3</i> )	0.3 ( <i>0.5</i> )*	0.8 (-0.3)
D4	0.4 ( <i>0.2</i> )	0.3 ( <i>1.4</i> )**	0.3 ( <i>1.1</i> )**	0.5 (-0.5)
D6	0.4 ( <i>0.4</i> )	0.3 ( <i>4.6</i> )**	0.4 ( <i>1.4</i> )**	0.5 (-0.7)*
D7	0.4 (-0.2)	0.3 ( <i>4.2</i> )**	0.4 ( <i>1.5</i> )**	0.6 (-2.4)**
MD10	0.6 (-0.3)	0.2 (-3.6)**	0.3 ( <i>0.8</i> )**	1.3 (-0.3)*
P8	1.3 ( <i>2.4</i> )**	0.9 ( <i>2.4</i> )**	1.3 ( <i>3.1</i> )**	1.9 ( <i>2.1</i> )**
<b>NH<sub>4</sub><sup>+</sup></b>				
C10	0.1 (-2.3)**	0 (-6.8)**	0.1 (-7.1)**	0.3 (-1.5)**
C3	0.2 ( <i>3.9</i> )**	0.2 ( <i>4</i> )**	0.3 ( <i>3.8</i> )**	0.2 ( <i>2.9</i> )**
D19	0.1 ( <i>0.4</i> )*	0 (-1.7)**	0 ( <i>1.2</i> )**	0.1 ( <i>2.5</i> )**
D26	0.1 ( <i>1.4</i> )**	0.1 ( <i>2.5</i> )**	0.1 ( <i>3.1</i> )**	0.1 ( <i>2.3</i> )**
D28	0.1 (-0.5)	0 (-3.7)**	0 (-1.6)**	0.1 ( <i>1.7</i> )**
D4	0.1 ( <i>1.7</i> )**	0 ( <i>1</i> )**	0 (-0.7)	0.1 ( <i>2</i> )**
D6	0.1 ( <i>2.9</i> )**	0.1 ( <i>2.8</i> )**	0.1 (-0.1)	0.1 ( <i>2.1</i> )**
D7	0.1 ( <i>3.3</i> )**	0 ( <i>2</i> )**	0.1 (-2.8)**	0.1 ( <i>1.7</i> )**
MD10	0.1 (-1.8)**	0 (-6.5)**	0 (-3.3)**	0.2 ( <i>0.4</i> )
P8	0.2 ( <i>3.9</i> )**	0.1 ( <i>1.8</i> )**	0.2 ( <i>7</i> )**	0.6 ( <i>7</i> )**
<b>NO<sub>2</sub><sup>-</sup>/NO<sub>3</sub><sup>2-</sup></b>				
C10	1.1 ( <i>1.5</i> )**	1.2 ( <i>0.6</i> )**	1.2 ( <i>1.3</i> )**	1.5 ( <i>1.8</i> )**
C3	0.2 ( <i>0.7</i> )**	0.1 (-1)**	0.1 (-0.3)	0.2 ( <i>1</i> )**
D19	0.4 ( <i>0.4</i> )	0.2 (-0.3)	0.3 ( <i>0.3</i> )	0.6 (-0.9)*
D26	0.4 ( <i>0.6</i> )*	0.2 (-0.1)	0.3 ( <i>0.3</i> )*	0.5 (-0.3)
D28	0.5 ( <i>0.7</i> )*	0.2 (-0.1)	0.3 ( <i>0.2</i> )	0.7 (-1)**
D4	0.3 ( <i>0.1</i> )	0.3 ( <i>1.4</i> )**	0.3 ( <i>1.1</i> )**	0.4 (-0.8)*
D6	0.4 (-0.2)	0.3 ( <i>4.1</i> )**	0.3 ( <i>1.4</i> )**	0.4 (-1)**
D7	0.4 (-1)*	0.3 ( <i>3.4</i> )**	0.4 ( <i>0.4</i> )	0.4 (-3.6)**
MD10	0.5 (-0.2)	0.2 (-3.6)**	0.2 ( <i>1.5</i> )**	1.2 (-0.5)*
P8	1.2 ( <i>2</i> )**	0.9 ( <i>2.3</i> )**	1.1 ( <i>2</i> )**	1.4 ( <i>1</i> )**

Summaries are medians (mg L<sup>-1</sup>) and percent change per year in parentheses (increasing in bold-italic). Changes and significance estimates are based on seasonal Kendall tests of flow-normalized results within each time period. Months for each season are Spring: MAM, Summer: JJA, Fall: SON, Winter: DJF. \* $p < 0.05$ ; \*\* $p < 0.005$

Table 3: Summaries of flow-normalized trends in nitrogen analytes for all stations and seasonal aggregations from 1996-2013

Analyte/Station	Seasonal, 1996-2013			
	Spring	Summer	Fall	Winter
<b>DIN</b>				
C10	1.1 (-4.1)**	1.3 (-3.1)**	1.6 (-2)**	1.7 (-3.4)**
C3	0.5 ( <b>0.5</b> )	0.4 ( <b>0.1</b> )	0.6 (-0.2)	0.5 (-0.6)**
D19	0.5 (-2.8)**	0.2 (-1)*	0.3 (-1.6)**	0.7 (-2.3)**
D26	0.5 (-1.9)**	0.3 (-1.7)**	0.4 (-1)**	0.6 (-0.8)**
D28	0.5 (-3)**	0.2 (-4.9)**	0.2 (-4.9)**	0.7 (-2.1)**
D4	0.4 ( <b>0</b> )	0.4 (-1)**	0.4 (-0.9)**	0.5 ( <b>0.6</b> )**
D6	0.5 (-0.2)*	0.5 (-1)**	0.5 (-0.3)*	0.5 (-0.1)
D7	0.5 (-0.8)**	0.4 (-1.3)**	0.4 (-0.4)**	0.6 (-0.2)
MD10	0.4 (-2.3)**	0.2 (-3.7)**	0.2 (-4.4)**	1 (-1.8)**
P8	1.5 (-1.9)**	1.2 (-3.5)**	1.8 (-2.4)**	2.7 (-2.2)**
<b>NH<sub>4</sub><sup>+</sup></b>				
C10	0 (-4.2)**	0 (-6.1)**	0 (-8.5)**	0.1 (-7.3)**
C3	0.3 ( <b>1</b> )**	0.3 (-0.8)*	0.4 (-0.5)*	0.2 (-0.1)
D19	0 (-1.9)**	0 (-0.4)	0 (-2.2)**	0.1 (-1.8)**
D26	0.1 (-1.2)**	0.1 (-1.3)**	0.1 (-1.9)**	0.1 (-1.4)**
D28	0 (-1.7)**	0 (-0.2)	0 (-2.4)**	0.1 (-3.1)**
D4	0.1 ( <b>0.3</b> )	0 (-1.3)**	0.1 (-0.3)	0.1 ( <b>1</b> )**
D6	0.1 (-0.7)**	0.1 (-1)**	0.1 ( <b>0.3</b> )	0.1 (-0.3)**
D7	0.1 (-2.2)**	0 (-2.1)**	0.1 ( <b>1.3</b> )**	0.1 (-0.4)*
MD10	0 (-1.4)*	0 (-0.1)	0 (-0.8)**	0.1 (-4.3)**
P8	0.2 (-8.7)**	0.1 (-6.3)**	0.2 (-10.4)**	0.5 (-13.1)**
<b>NO<sub>2</sub><sup>-</sup>/NO<sub>3</sub><sup>2-</sup></b>				
C10	1.1 (-4.2)**	1.2 (-3.2)**	1.6 (-1.9)**	1.6 (-3.3)**
C3	0.2 ( <b>0.4</b> )	0.1 ( <b>3.1</b> )**	0.2 ( <b>1.7</b> )**	0.2 (-0.4)
D19	0.4 (-2.9)**	0.2 (-1)*	0.3 (-1.5)**	0.6 (-2.2)**
D26	0.4 (-1.9)**	0.2 (-1.6)**	0.3 (-0.6)*	0.5 (-0.6)**
D28	0.5 (-3)**	0.2 (-5.4)**	0.2 (-5.2)**	0.7 (-1.7)**
D4	0.3 (-0.1)	0.3 (-1)**	0.3 (-1)**	0.4 ( <b>0.4</b> )**
D6	0.4 (-0.1)	0.4 (-1)**	0.4 (-0.4)*	0.4 (-0.1)
D7	0.4 (-0.6)**	0.4 (-1.2)**	0.4 (-0.8)**	0.4 (-0.3)*
MD10	0.4 (-2.6)**	0.1 (-4.5)**	0.2 (-5.4)**	1 (-1.4)**
P8	1.3 (-1.1)**	1.1 (-3.1)**	1.6 (-0.3)*	2.2 ( <b>0</b> )

Summaries are medians (mg L<sup>-1</sup>) and percent change per year in parentheses (increasing in bold-italic). Changes and significance estimates are based on seasonal Kendall tests of flow-normalized results within each time period. Months for each season are Spring: MAM, Summer: JJA, Fall: SON, Winter: DJF. \* $p < 0.05$ ; \*\* $p < 0.005$

Table 4: Summaries of flow-normalized trends in nitrite/nitrate and ammonium ( $\text{mg L}^{-1}$ ) concentrations before and after WWTP upgrades upstream of station P8

Period	$\text{NO}_2^-/\text{NO}_3^{2-}$		$\text{NH}_4^+$	
	Median	% change	Median	% change
<b>Annual</b>				
1976-2006	1.3	<b>2**</b>	0.2	<b>2.8**</b>
2007-2013	1.4	-1.9**	0.1	-16.6**
<b>Seasonal, pre</b>				
Spring	1.2	<b>1.6**</b>	0.2	<b>1.4**</b>
Summer	1	<b>2.4**</b>	0.1	<b>3.3**</b>
Fall	1.3	<b>2.2**</b>	0.2	<b>4.9**</b>
Winter	1.5	<b>2.1**</b>	0.7	<b>4.8**</b>
<b>Seasonal, post</b>				
Spring	1.3	-1.6**	0.1	-16.2**
Summer	0.9	-4.3**	0.1	-15.7**
Fall	1.5	-1.7**	0.1	-19.3**
Winter	2.2	-0.8**	0.2	-26.7**

Upgrades were completed in 2006 at the City of Stockton WWTP (San Joaquin County, Fig. 7). Summaries are medians and percent change per year in parentheses (increasing in bold-italic). Changes and significance estimates are based on seasonal Kendall tests of flow-normalized results within each time period. Increasing values are in bold-italics. Months for each season are Spring: MAM, Summer: JJA, Fall: SON, Winter: DJF. \* $p < 0.05$ ; \*\* $p < 0.005$